

International Journal of Sustainable Engineering

ISSN: 1939-7038 (Print) 1939-7046 (Online) Journal homepage: www.tandfonline.com/journals/tsue20

Pyrolysis of aircraft cabin materials for chemical recycling

Clemens Schmittmann , Kai Schlögel , Fabian Roemer , Kevin Carl & Peter Quicker

To cite this article: Clemens Schmittmann , Kai Schlögel , Fabian Roemer , Kevin Carl & Peter Quicker (2026) Pyrolysis of aircraft cabin materials for chemical recycling, International Journal of Sustainable Engineering, 19:1, 2735274, DOI: 10.1080/19397038.2026.2735274

To link to this article: https://doi.org/10.1080/19397038.2026.2735274

© 2026 The Author(s). Published by Informa UK Limited, trading as Taylor & Francis Group.

Published online: 24 Sep 2026.

Submit your article to this journal

Article views: 238

View related articles

View Crossmark data

Full Terms & Conditions of access and use can be found at
https://www.tandfonline.com/action/journalInformation?journalCode=tsue20

INTERNATIONAL JOURNAL OF SUSTAINABLE ENGINEERING
2026, VOL. 19, NO. 1, 2735274
https://doi.org/10.1080/19397038.2026.2735274

Taylor & Francis
by informa

RESEARCH ARTICLE

OPEN ACCESS Check for updates

Pyrolysis of aircraft cabin materials for chemical recycling

Clemens Schmittmann[a], Kai Schlögel[a], Fabian Roemer[b], Kevin Carl[a] and Peter Quicker[a]

[a]Thermoprocesses and Emission Control in Waste Management and Recycling Teaching and Research Unit, RWTH Aachen University, Aachen, Germany; [b]Formerly a, Currently REMONDIS Recycling GmbH & Co. KG, Lünen, Germany

ABSTRACT

Increased usage of high-performance composite materials results in the necessity of novel routes of recycling for these materials. This article focuses on the application of pyrolysis for the recovery of potentially reusable carbon-based molecules from artificially aged aircraft components. Two different fractions of Ultem 1000-based components and one Nomex-based sample were pyrolysed, and the resulting chars, oils and gases were comprehensively characterised. Owing to the great heat resistance of the materials tested, the majority of the products obtained were chars and pyrolysis gases, and the proportion of condensable oils was very low. The condensates showed a highly complex composition, indicating their limited suitability for direct material recovery via pyrolysis oil utilisation under the investigated conditions. At the same time, the results provide insight into the decomposition behaviour of thermally stable polymers and highlight key constraints for the thermochemical treatment of such waste streams, including low condensable product yields, high product heterogeneity and the occurrence of halogen-containing species. Overall, this study identifies important limitations of direct pyrolytic recycling for these aircraft cabin materials and provides a basis for discussing alternative recovery strategies, process adaptations and design considerations for improved circularity.

ARTICLE HISTORY
Received 9 February 2026
Accepted 13 September 2026

KEYWORDS
Pyrolysis; circular economy; chemical recycling; aircraft cabin materials; feasibility assessment

1. Introduction

The increasing use of high-performance polymer composites in the aviation industry has significantly improved fuel efficiency and passenger safety, but has also created new challenges for end-of-life (EoL) management (Bachmann et al. 2021). Aircraft cabin components, such as side panels, clips, and interior structures, often consist of fibre-reinforced thermosets or thermoplastics with complex multilayer architectures (National Research Council 1995). Their composition, which typically involves phenolic resins, polyetherimides, and glass or aramid fibres, limits the applicability of conventional mechanical recycling. In many cases, landfilling or incineration remains the dominant disposal route, leading to a permanent loss of valuable carbon resources and potential emissions of hazardous degradation products (Qureshi 2022).

Thermochemical conversion technologies, such as pyrolysis, represent a potential pathway for the recovery of carbon-rich residues and volatile organic compounds from composite materials at the end of their life. By applying an oxygen-free atmosphere, polymeric matrices can be decomposed into condensable organic fractions, permanent gases, and solid carbonaceous residues (Pahnila et al. 2023). These product streams can serve as feedstocks for chemical recycling or energy recovery, depending on their composition and purity (Qureshi 2022). However, the complex chemical nature of aircraft cabin composites poses significant challenges for process control, emission mitigation, and downstream utilisation of the resulting products (Naqvi et al. 2018). Moreover, the presence of glass or aramid fibres, thermally stable additives, and flame retardants affects both decomposition kinetics and product yields (Yousef et al. 2021).

Compared with mechanical recycling, pyrolysis generally shows a higher tolerance toward heterogeneous and mixed polymer waste streams. However, the original polymer structure is thermally decomposed, and

CONTACT Clemens Schmittmann clemens.schmittmann@rwth-aachen.de

© 2026 The Author(s). Published by Informa UK Limited, trading as Taylor & Francis Group.
This is an Open Access article distributed under the terms of the Creative Commons Attribution License (http://creativecommons.org/licenses/by/4.0/), which permits unrestricted use, distribution, and reproduction in any medium, provided the original work is properly cited. The terms on which this article has been published allow the posting of the Accepted Manuscript in a repository by the author(s) or with their consent.

the contribution of pyrolysis to circular resource use therefore strongly depends on the recovery, upgrading and subsequent utilisation of the resulting solid, liquid and gaseous products (Clark and Shaver 2024; Luo et al. 2024). Mechanical recycling may preserve material value in cleaner and separable fractions, but is strongly limited for multilayer aircraft cabin components because of adhesives, fibre reinforcement, contamination and reduced product quality. Incineration or cement-kiln co-processing remains technically robust for heterogeneous composite waste and enables energy recovery, but leads to an irreversible loss of material resources (Qureshi 2022). Solvent-based or solvolytic approaches may be more suitable for comparatively clean thermoplastic fractions, whereas gasification may be more relevant when product-gas recovery is prioritised. Pyrolysis should therefore be assessed as one option within a broader end-of-life strategy rather than as a universally preferable recycling route.

While pyrolysis of conventional plastics and biomass-derived polymers has been extensively investigated, only limited data is available on the thermal degradation behaviour of aircraft-specific interior materials under controlled inert conditions (Wong et al. 2017). A detailed understanding of their devolatilization and product formation behaviour is essential for evaluating the feasibility and limitations of thermochemical recycling pathways and for minimising the environmental footprint associated with end-of-life aircraft components.

This study, therefore, investigates the pyrolysis of two artificially aged aircraft cabin components, a fibre-reinforced phenolic composite and a glass fibre-reinforced polyetherimide (Ultem 1000), and compares their thermal conversion behaviour to that of a virgin-grade Ultem 1000 reference. The focus lies on characterising product yields, gas compositions, and condensate properties to assess the feasibility and limitations of pyrolysis-based recycling as well as the emission behaviour of these materials under defined process conditions. The experiments were carried out in a laboratory-scale muffle furnace equipped with an inert gas supply and product gas condensation system. The results provide insights into the decomposition behaviour of aircraft cabin polymers and contribute to the evaluation of thermochemical treatment routes for these materials in the context of circular end-of-life management and alternative recovery strategies in the aviation sector.

2. Materials and methods

2.1. Materials

Three different materials were used in this study: two being artificially aged aircraft cabin components and one virgin-grade reference material. The first cabin component consisted of side panels made of a Nomex honeycomb base lined with glass-fibre reinforcement and impregnated with a phenolic resin. The second component is a mixture of the corresponding retaining clips from the side panels, consisting of glass fibre-reinforced Ultem 1000. These retaining clips were glued to the backs of the side panels. The separation of both materials was conducted manually. The reference material used was virgin-grade Ultem 1000. Owing to size restrictions, the side panels were manually cut into pieces of approximately 10×10 cm prior to the experiments. Pictures of the materials used are displayed in Figure 1.



Figure 1. Samples used in this study. Left: EoL side-panels, middle: EoL retaining clips, right: reference material.

The cabin components were provided by Diehl Aviation Laupheim GmbH (Laupheim, Germany) and represent real, state-of-the-art cabin components. Prior to the experiments, they were artificially aged in the company's own laboratory. First, the components were heated to 85 °C ±3°C for 500 h ±2 h and then cooled to 23 °C for 24 h. Then, the parts were heated to 85 °C ±2 °C for another 500 h ± 2 h at a relative humidity of 95% ±5%. After cooling down to room temperature, the parts were tested in an alternation test in which the parts were heated to 85 °C for 30 min and then cooled down to −55 °C for 30 min with a heat up/cool down rate of 2 K/min. This alternation test was conducted three times. The conditions of the artificial ageing are displayed in Table 1.

The samples were analysed regarding their chemical and immediate composition. The results are displayed in Table 2. The chemical composition of the samples is as expected for the polymer type contained in the corresponding samples. The retaining clips, as well as the cabin side panels, contained large amounts of glass fibres, resulting in high ash contents of 30.1% for the retaining clips and 53.3% for the cabin side panels.

2.2. Muffle furnace

All pyrolysis experiments were performed in a laboratory-scale muffle furnace (KM 70/13, Thermconcept GmbH, Germany) designed for high-temperature batch operation under an inert atmosphere. The furnace has an electrical heating capacity of 20 kW and allows operation up to 1,200 °C. Heating is achieved by three independent circuits, two located along the sidewalls and one at the bottom of the chamber, ensuring a homogeneous temperature distribution within the furnace. The furnace chamber was lined with refractory bricks for thermal insulation and stability during high-temperature operation.

A rectangular stainless-steel retort was used to contain the samples during the experiments. The retort measures approximately $500 \times 300 \times 180$ mm and is equipped with a perforated bottom plate that distributes the incoming purge gas evenly beneath the sample bed. Two thermocouple ports allow continuous temperature measurement inside the retort, one positioned near the centre and a second inserted through a sleeve to capture axial temperature gradients.

Inert gas (nitrogen, grade 5.0) was introduced from below the sample bed at a constant flow rate of approximately 500 L h^{-1}. The evolving pyrolysis gases were continuously removed through an outlet located at the upper section of the retort and transferred via a heated stainless-steel line (2″ diameter, maintained at ~300 °C) to two stainless-steel, impinger-style condensate traps placed in a cooling bath at −30 °C, followed by the gas analysis and afterburning units.

The muffle furnace setup enables well-defined and reproducible thermal conditions, with a maximum process temperature of 700 °C applied in this study. This configuration provides a reliable platform for investigating the devolatilization and gas formation behaviour of composite materials under inert

Table 1. Test cycles for the artificial ageing of the cabin materials used.

Condition before testing	23 °C for 72 h		
Test conditions	Cycle 1 (heat)	Cycle 2 (humidity)	Cycle 3 (alternation)
Temperature [°C]	85 ± 3	85 ± 2	85 to −55 at 2 K/min
Humidity [r.H., %]	–	95 ± 5	–
Time [h]	500 ± 2	500 ± 2	0.5 | 3 cycles

Table 2. Feedstock ultimate and proximate analyses.

		Retaining clip	Ultem 1000 Reference	Cabin side panel	Standard
Base polymer		Ultem 1000	Ultem 1000	Nomex/phenolic resin	–
Fiber reinforced		Glass fiber	No	Glass fiber	–
Water	[%]	0.4	0.7	0.9	DIN EN ISO 18134-3
Ash		30.1	0.28	53.3	DIN 51719
C		52.8	75.1	34.1	DIN 51732
H		2.9	3.9	2.8	DIN 51732
N		1.8	2.5	1.2	DIN 51732
S		<0.02	<0.02	<0.02	DIN 51724
Cl		<0.1	<0.2	0.3	DIN 51727
LHV	[MJ/kg]	20.1	28.3	12.7	DIN 51900

atmospheres. A schematic representation of the experimental setup, including the furnace, retort and gas handling system, is shown in Figure 2.

2.3. Characterisation of products

The pyrolysis gases produced during the experiments were directed through two condensation traps, being placed in a cold bath at −30 °C. The condensates formed in each of the condensation traps were manually removed after the experiments and stored in brown glass bottles with PTFE seals. The samples were stored at −20 °C before being subjected to GC-MS analysis. Three different GC-MS measurements were conducted for each sample in order to achieve the best measurement conditions for each group of components. First, the samples were diluted with a mixture of methanol/dichloromethane (1:1) at a ratio of 1:10 to 1:100, depending on the specific properties of the sample. Then, the first analysis was conducted, being a non-target analysis to obtain general information regarding the corresponding sample composition as well as concentrations. Afterwards, a specific scan was conducted targeting the concentrations of benzene, toluene, ethylbenzene and xylenes. The final scan targeted 16-EPA-PAK. The non-target GC–MS measurements were primarily used for qualitative characterisation of the condensates and for identifying the dominant compound classes. Owing to the high complexity of the samples, the resulting chromatograms were not interpreted as a fully quantitative compositional analysis. The quantitative assessment was therefore limited to the targeted compounds analysed separately (BTEX, BPA and 16-EPA-PAK). Furthermore, the condensates were analysed regarding their hydrogen, carbon and nitrogen content. Because of the low sample amounts, high volatility and possible phase inhomogeneity of the condensates, the elemental analysis of the liquid fractions was interpreted as indicative.

The chars obtained from the experiments were manually removed from the retort, roughly crushed if necessary and stored in plastic containers before being analysed at the institute laboratory. Analysis performed was ultimate and proximate analysis, as well as XRF-spectroscopy.

Characterisation of the remaining gases after condensation was carried out with a variety of different analysers and methods. All the measurements were done in cooled product gas (approximately 0 °C) after condensation. So-called permanent gases such as O_2, H_2, CO, CO_2 and CH_4 were measured using a multigas-measurement device (VISIT 03 H, Messtechnik EHEIM GmbH, Schwaigern, Germany), using

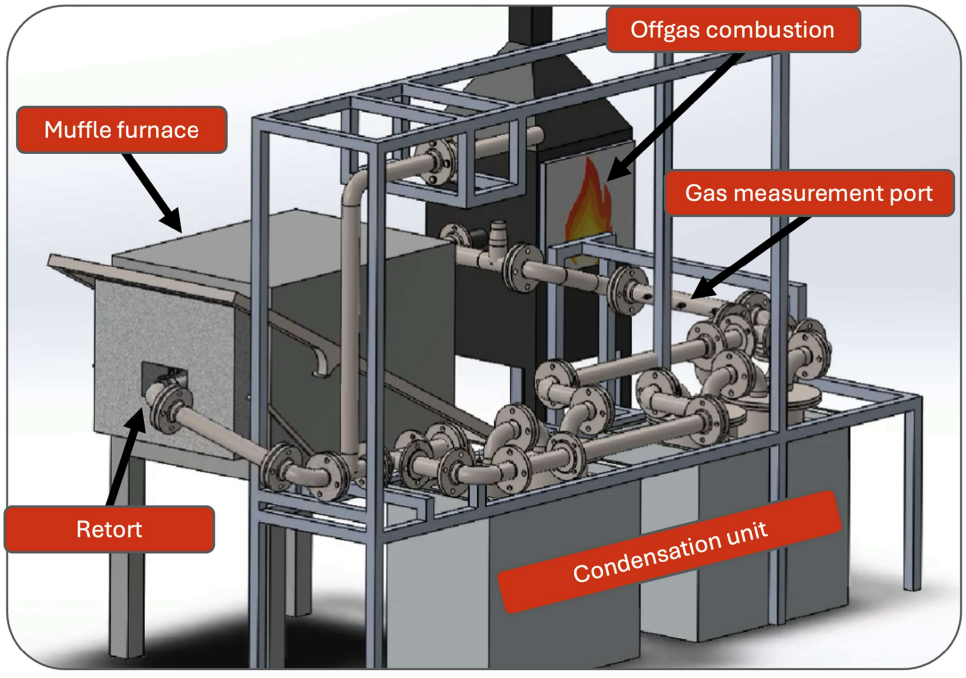


Figure 2. Schematic representation of the experimental setup used in this study. The pipe layout at the condensation traps allows switching between single and double condensation as well as bypass operation.

NDIR (CO, CO_2, CH_4), TCD (H_2) and electrochemical (O_2) sensors. In order to protect the sensors of the device, a sample gas preparation was used. First, the sample gas is washed using a washing oil and water, then it is cooled down to approximately 5 °C, passed through silica gel, activated carbon and a series of filters. Furthermore, the product gases were analysed using an FTIR (CX4000, Gasmet Technologies GmbH, Karlsruhe, Germany), obtaining selected components, such as hydrocarbons (C_1–C_6), acid gases and nitrogen oxides. As the total concentration of IR-active sample gas components was expected to be too high, the sample gas was diluted using pure nitrogen. This was done to prevent a phenomenon called total absorption, where the gas is so IR active that it absorbs all the light from the IR source in the FTIR, making it impossible to characterise the gas. Additionally, gas components that occur in smaller concentrations cannot be detected in the resulting spectra of undiluted sample gases because of broadening of the CO, CO_2 and H_2O peaks at high concentrations due to overlapping. Therefore, a volumetric dilution of 1:10 (sample gas to nitrogen) was used. The exact dilution was measured by an internal diluting device via pressure sensors. The sample was taken via a heated sample line (180 °C) that was connected to a series of heated quarzwool-filters, which were used to protect the device from dust or condensing tars from the sample gas. A schematic representation of the measurement setup is given in Figure 3.

3. Experimental procedure

The sample was placed into the retort and evenly distributed on a metal mesh, preventing smaller particles from falling on the bottom of the retort. For all the experiments, 400 g of sample mass was used except for the mounting clips, where 200 g of sample was used because of the limited amounts available. The retort was closed and placed into the muffle furnace. The setup was tested for leakages, and after a successful test, the sample was heated to 700 °C with a heating ramp of approximately 3–5 K min^{-1}. During the experiment, the retort was purged with approximately 500 L h^{-1} nitrogen (grade 5.0). After reaching 700 °C, the samples remained at that temperature for 60 minutes before cooling down overnight. The resulting chars were removed from the retort and analysed, and the produced condensates were removed from the condensate traps and stored separately in brown glass containers with PTFE seals at −20 °C before being sent off for analysis. All products obtained (char, condensates) were weighed. All the experiments were conducted twice to verify the results obtained. The duplicate experiments were primarily used to assess the reproducibility of the general product yield distribution and the overall gas-evolution trends. Local deviations in individual gas concentration profiles were evaluated with caution and are discussed in the corresponding sections.

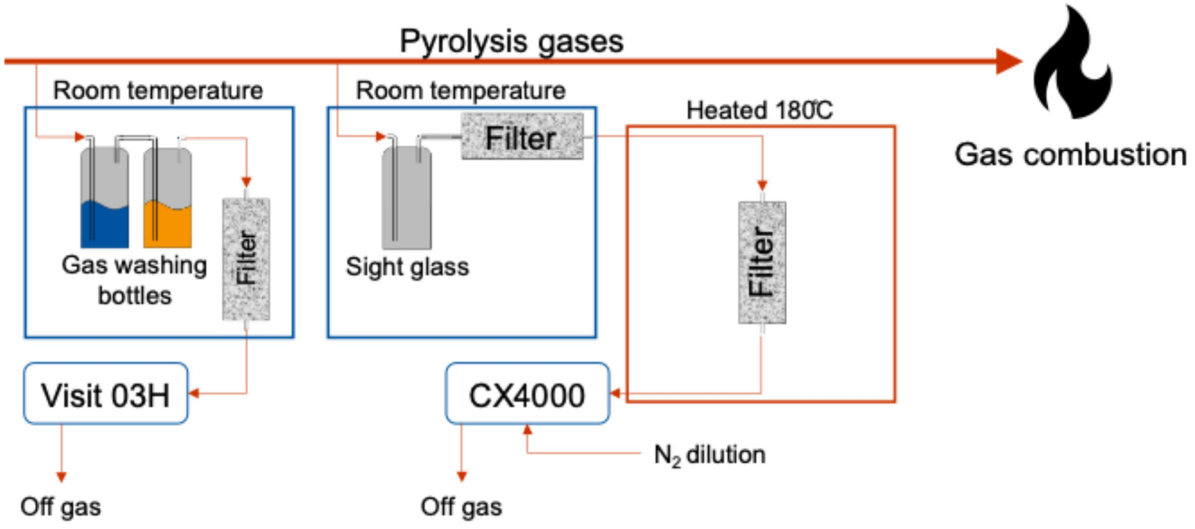


Figure 3. Schematic representation of pyrolysis gas measurement.

4. Results and discussion

When focusing on the overall yield distribution, as displayed in Figure 4, all samples showed similar behaviour. As two condensation traps were used, individual yields are given for each trap. The majority of the products obtained were char with the highest yields obtained by both cabin parts (mounting clip and side panel), with approximately 70% yield. The reference material investigated showed lower char-forming tendencies, probably due to the lack of glass-fibre enforcement. When normalised to an ash-free state, the tendencies for char formation and gas evolution are almost identical for the Ultem 1000-based samples (char formation: 0.56–0.63 g g^{-1} ($m_{char_{ash\,free}}/m_{sample_{ash\,free}}$); gas formation: 0.33–0.36 g g^{-1} ($m_{gas}/m_{sample_{ash\,free}}$)). When focusing on the side panels investigated, the char formation was significantly lower with values of approximately 0.38–0.40 g g^{-1} ($m_{char_{ash\,free}}/m_{sample_{ash\,free}}$), but the gas formation was higher with values of approximately 0.48–0.52 g g^{-1} ($m_{gas}/m_{sample_{ash\,free}}$). All the samples showed a minor production of pyrolysis oils with about 4%–8.2%. When compared to the ash-free sample mass, condensate formation yielded values of approximately 0.07–0.14 g g^{-1} ($m_{condensates}/m_{sample_{ash\,free}}$).

4.1. End-of-life retaining clips

The degassing behaviour of the end-of-life retaining clips is displayed in Figure 5, and focuses on the permanent gases. As expected for high-temperature-resistant plastics, no decomposition of the sample can be observed until reaching temperatures above approximately 360 °C. Before that, only minor amounts of CO_2 could be observed to degas from the sample. After exceeding the decomposition temperature, a strong increase in CH_4, CO and CO_2 concentrations can be observed. Only after reaching temperatures above approximately 500 °C was the formation of H_2 observed. The maximum concentration of CH_4 and CO_2 was reached at approximately 550 °C. CO and H_2 concentrations peaked later at approximately 650 °C. The early formation of CO_2 and CO can be attributed to the cleavage of oxygen-containing structural units and carbonyl-type functionalities, whereas CH_4 is likely formed by the cracking of methyl-containing side groups and smaller aliphatic fragments. The delayed formation of H_2 at higher temperatures indicates secondary cracking and dehydrogenation reactions of already formed pyrolysis intermediates. A distinct deviation between both duplicate experiments can be observed in the CO, CO_2 and CH_4 signals at approximately 100 min. This discrepancy is temporally limited and may be related to a short-term problem

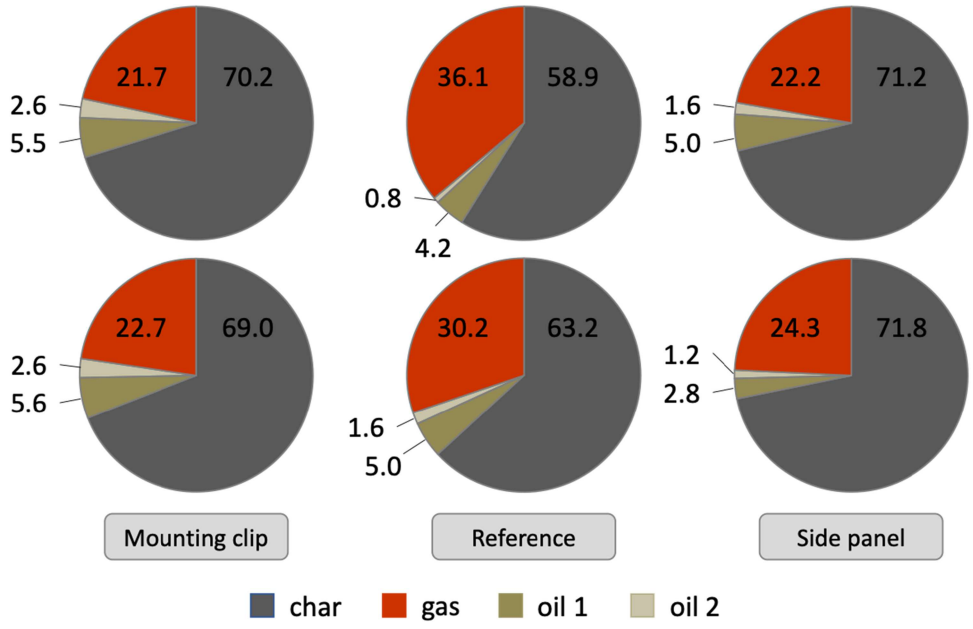


Figure 4. Yield distribution for the experiments conducted. Oil 1 and oil 2 represent the amount of pyrolysis oil found in condensation traps 1 and 2, respectively. All values are in [%].

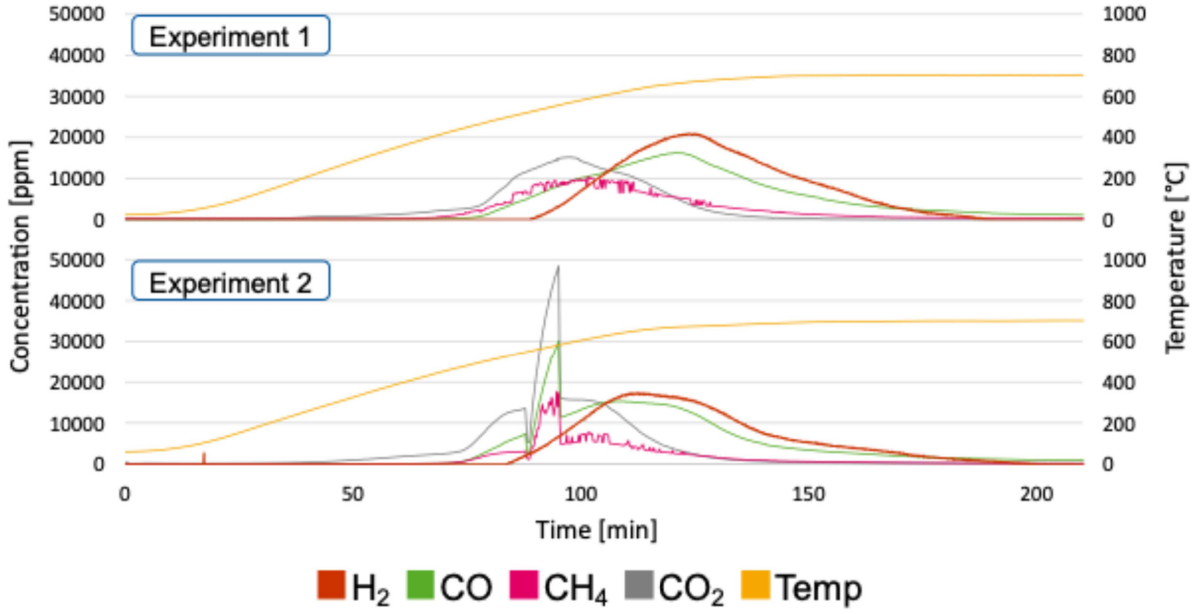


Figure 5. Degassing behaviour of the EoL retaining clips during the experiments. The reference state is dry for all the gas components.

in the gas measurement. Since the overall gas-evolution pattern remains comparable between both experiments, the general interpretation of the devolatilization behaviour is considered robust. However, the absolute peak intensities in this time interval should be interpreted with caution.

When focusing on other gas components detected via FTIR, a variety of decomposition products can be observed. Figure 6 displays selected components obtained from the measurement. The most prominent components were toluene and pyridine, followed by propene, benzene and xylene as well as NH_3, HCN and propane. While the concentrations of these substances highly vary, with concentrations of approximately 300 ppm to 37,000 ppm, they are all released from the sample at very similar temperatures, starting at approximately 300 °C. The formation of propane and propene indicates that, besides aromatic fragments, small hydrocarbons are generated during pyrolysis by the cleavage of aliphatic side groups and by the secondary cracking of larger volatile fragments. While C_3-fragments could be observed, the amount of ethylene and ethyne formed in the experiments was low, with values below 120 ppm. No significant formation of ethane was observed. Nitrogen-containing species such as NH_3, HCN and pyridine are consistent with the decomposition of nitrogen-bearing polymer structures in the Ultem-based material. In addition, the formation of HCl was observed in the FTIR spectra at temperatures above 400 °C. Although only low chlorine contents were measured in the feed material (see Table 2), this finding indicates the presence of chlorine-containing constituents or residues in the investigated material system. Based on the available data, however, the exact origin of the HCl signal cannot be assigned unambiguously. To the best of our knowledge, no chlorine is supposed to be in the base material (polyetherimide) itself. Potentially, the chlorine detected resulted from residues of glue or paint on the EoL-parts.

The obtained pyrolysis oils contained almost no benzene, toluene, ethylbenzene and xylene (BTEX) for both fractions of the condensates. A minor amount of bisphenol A was detected (19.3–75.1 mg L^{-1}). Furthermore, the oils contained approximately 1.5–2.6 mg EPA-16-PAK. The highest concentrations of all these substances were found in the condensate from the first condensation unit.

The chromatograms of the condensates were manually evaluated and displayed the fragmentation pattern of the end-of-life retaining clips. Owing to the large variety of substances possibly involved in thermochemical degradation, the chromatograms were primarily used to show the fragmentation pattern and to identify the dominant compound classes present in the condensate. The chromatograms of the pyrolysis oils obtained from the first experiment are displayed in Figures 7 and 8. Owing to the similarity of the chromatograms obtained from the first experiment with those from the validation measurement,

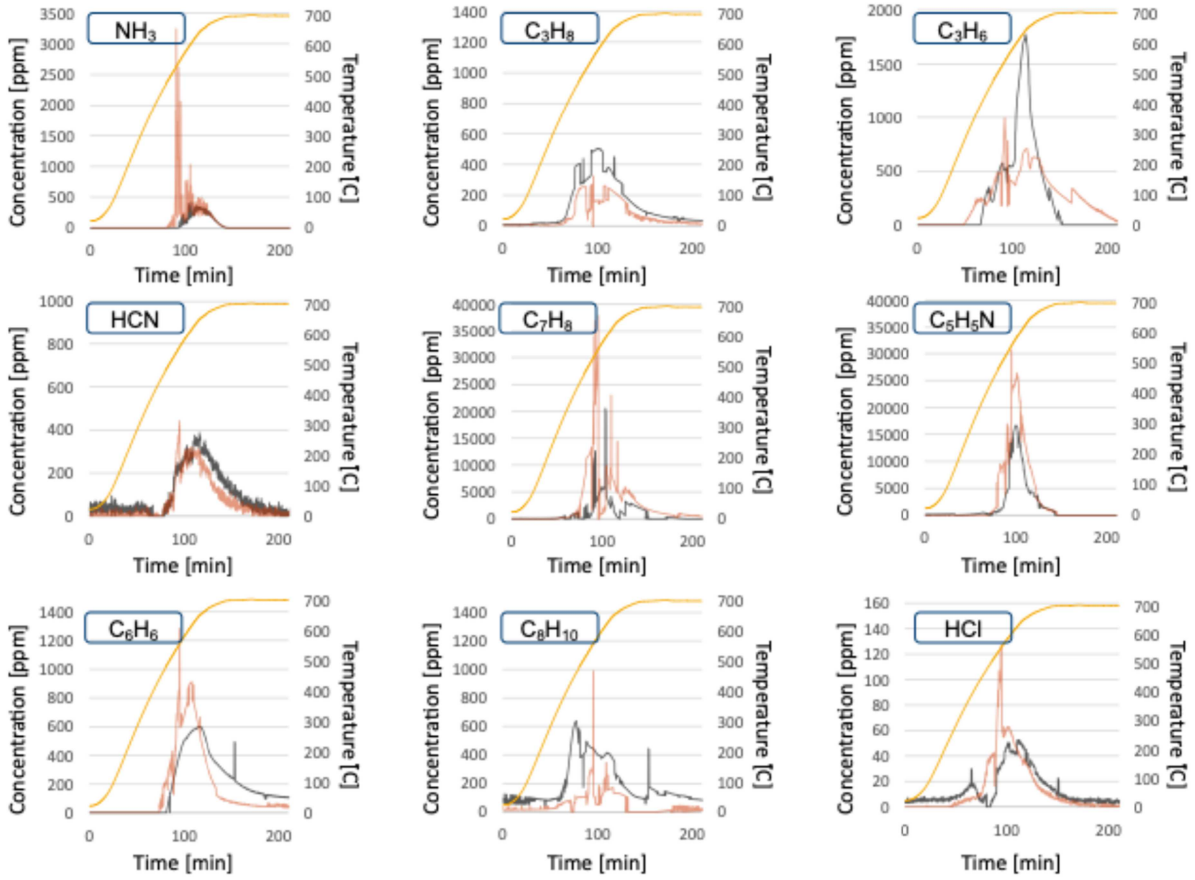


Figure 6. Minor gas components were detected via FTIR for the EoL retaining clips. The reference state is dry for all the gas components. Red: Experiment 1, grey: Experiment 2, yellow: temperature profile.

only the chromatograms from the first experiment are shown. This also applies to the subsequent experiments.

The first condensation unit yielded the majority of pyrolysis oils for both experiments conducted. Approximately 11 g of oil was recovered (exp. 1: 10.96 g, exp. 2: 11.3 g). The majority of substances found were benzene-based molecules with characteristic structural groups such as amines, nitriles and hydroxides. Furthermore, larger molecules such as biphenyls, a variety of diphenylethers, cumylphenols and phthalimides were observed (see Figure 7). All of these molecules seem to be characteristic degradation products of the polyetherimide used. Surprisingly, a distinctive peak at approximately 1,620 s was observed, representing bis(2-ethylhexyl)phthalate (no. 23), a commonly used plasticiser. It is unclear if this component originates from the sample itself or represents a contamination. The total number of peaks in the chromatogram of the first condensation unit was 2,192, displaying the vast amount of decomposition products formed. This broad compound distribution indicates a highly heterogeneous condensate composition and can be seen as a limiting factor for the material use of those pyrolysis oils.

The second condensation unit yielded approximately 5 g of condensates (exp. 1: 5.27 g, exp. 2: 5.26 g). The chromatograms of these samples contained significantly fewer peaks with a total of 776 (see Figure 8). This indicates that the majority of the components had already condensed in the previous condensation trap. As previously mentioned, the majority of the products identified were degradation products of the polyetherimide, but also a significant amount of (*p*-hydroxyphenyl)-phosphonic acid was found. This can be an indication for the use of phosphonic acid-based flame retardants, as this substance is commonly used as such (Sonnier et al. 2019; Stanfield et al. 2021; Zhou et al. 2020). However, the available analytical data do not allow assignment to a specific additive or flame-retardant formulation. Compared to the first condensation unit, the second condensate represented a smaller and less diverse fraction, but still consisted of a chemically heterogeneous mixture. Since the pyrolysis oils obtained were expected to have a highly

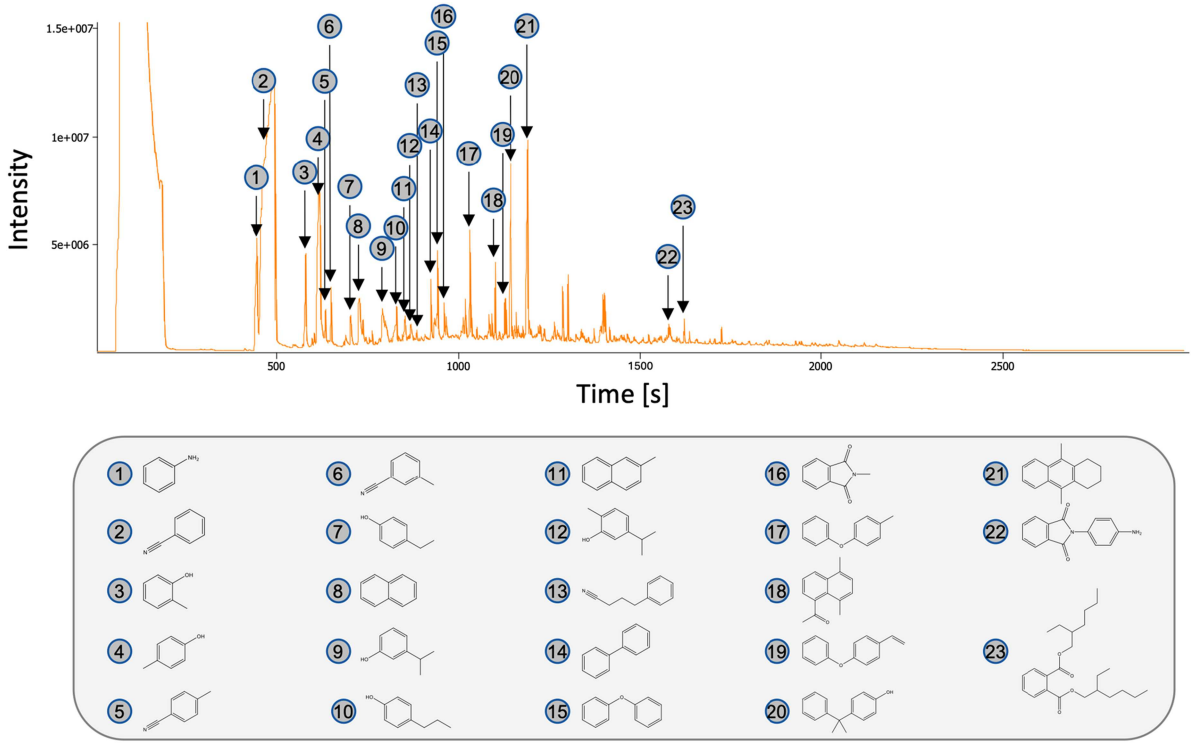


Figure 7. Chromatogram of the pyrolysis oil obtained from the retaining clips found in the first condensation trap.

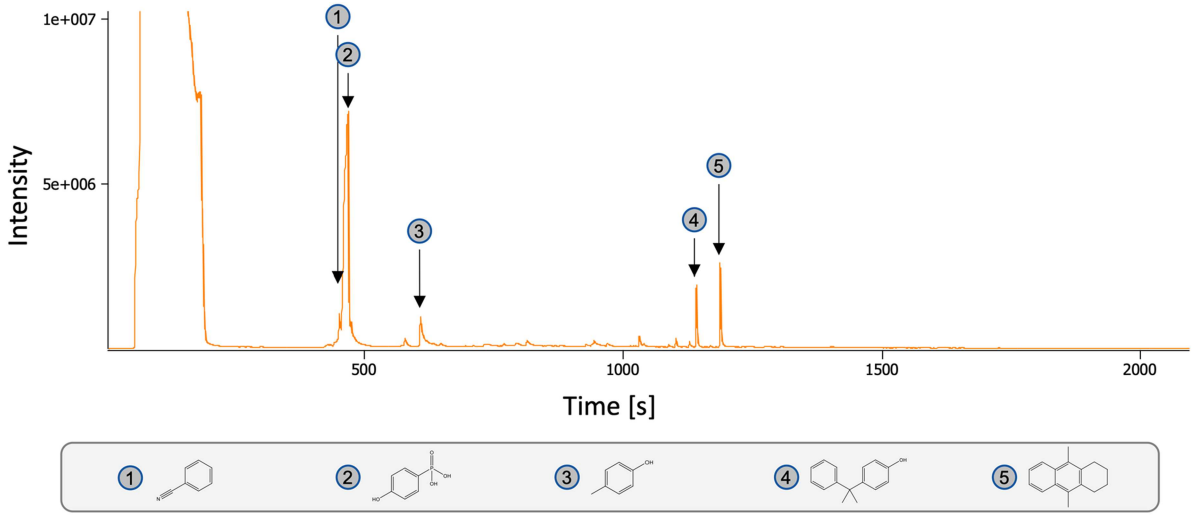


Figure 8. Chromatogram of the pyrolysis oil obtained from the retaining clips found in the second condensation trap.

heterogeneous composition, the elemental analysis of the condensates was conducted several times. This was intended to demonstrate the dispersion of the measured values and minimise errors in the subsequent interpretation of the data. While the hydrogen and nitrogen content is relatively similar for all samples (hydrogen: approximately 7%–9%, nitrogen: approximately 0.8%–3%), the amount of carbon is the largest in the pyrolysis oils of the first condensation trap. This indicates that the majority of the hydrocarbons condensed during this stage of condensation. The deviation of the values measured is, especially for carbon, relatively large, ranging from approximately 12% to 60%. This scatter indicates limited reproducibility of the elemental analysis for the condensate samples and may be related to sample volatility, phase inhomogeneity and challenges in handling small amounts of liquid product. Therefore, the carbon values

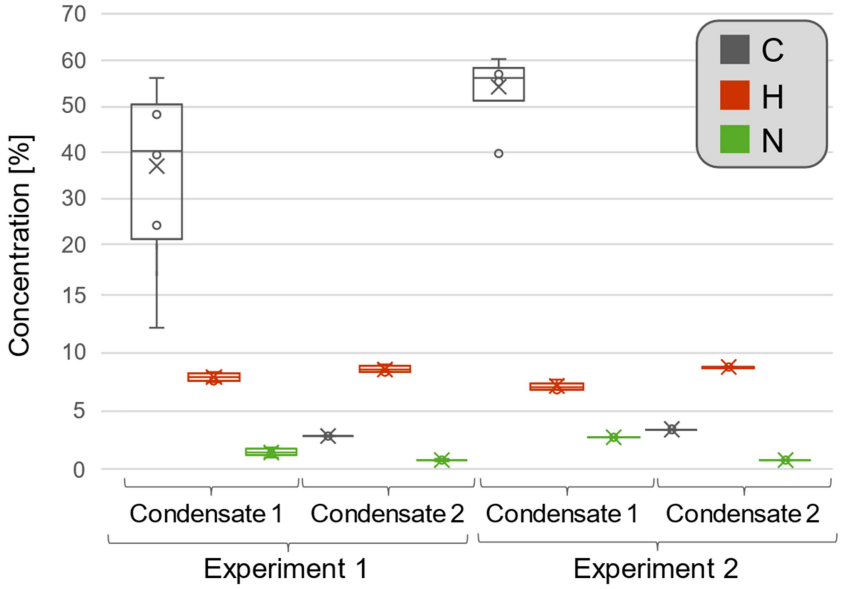


Figure 9. Ultimate analysis of the condensates produced by pyrolysis of the retaining clips. The values refer to the reference state wet.

should be interpreted with caution and mainly in a qualitative manner. The data obtained are displayed in Figure 9.

4.2. Virgin-grade Ultem 1000

The overall gas composition as well as its formation temperature are very similar compared to the end-of-life retaining clips. The main difference is that a higher gas concentration is obtained because of the greater amount of sample used (400 g per experiment). At first, a slight formation of CO_2 can be observed at temperatures exceeding approximately 300 °C. As observed in the previous experiment using the end-of-life retaining clips, the formation of CO and CH_4 can be observed at temperatures above approximately 360 °C. The formation of H_2 starts at temperatures above approximately 500 °C. This gas-evolution pattern again suggests initial cleavage of oxygen-containing groups with the formation of CO_2 and CO, followed by the release of CH_4 from smaller aliphatic fragments and side-group cracking. The latter increase in H_2 indicates secondary high-temperature reactions such as dehydrogenation and aromatisation of primary pyrolysis products. The permanent gas formation is displayed in Figure 10.

The fluctuations in the CH_4 content are likely an indication of limitations in the evaluation of the FTIR spectra. This phenomenon usually appears in highly complex gas mixtures, in which the automated evaluation of the spectra struggles to identify the corresponding peaks due to overlapping with peaks of other substances with similar IR-spectra. Accordingly, these short-term fluctuations were not interpreted as evidence of major changes in the overall decomposition behaviour, but rather as an analytical limitation of the spectral deconvolution under highly complex gas conditions.

Other components measured via FTIR are displayed in Figure 11 and show very similar behaviour compared to the results obtained from the end-of-life Ultem. The concentrations measured were higher as the sample mass for this experiment was doubled. Furthermore, the peak for NH_3 was broader, indicating a formation over a longer period of time. The data obtained for propane and toluene both show two peaks. It is unclear whether this is due to a two-step decomposition mechanism or indicates an incorrect computer-based evaluation of the FTIR-spectra. As the gap between both peaks is rather long (approximately 10 min), it is assumed to indicate a two-step-decomposition mechanism. The detection of propane in particular confirms that low-molecular-weight hydrocarbons are formed in addition to the permanent gases, most likely by the cleavage of aliphatic substituents and secondary cracking of larger volatile species.

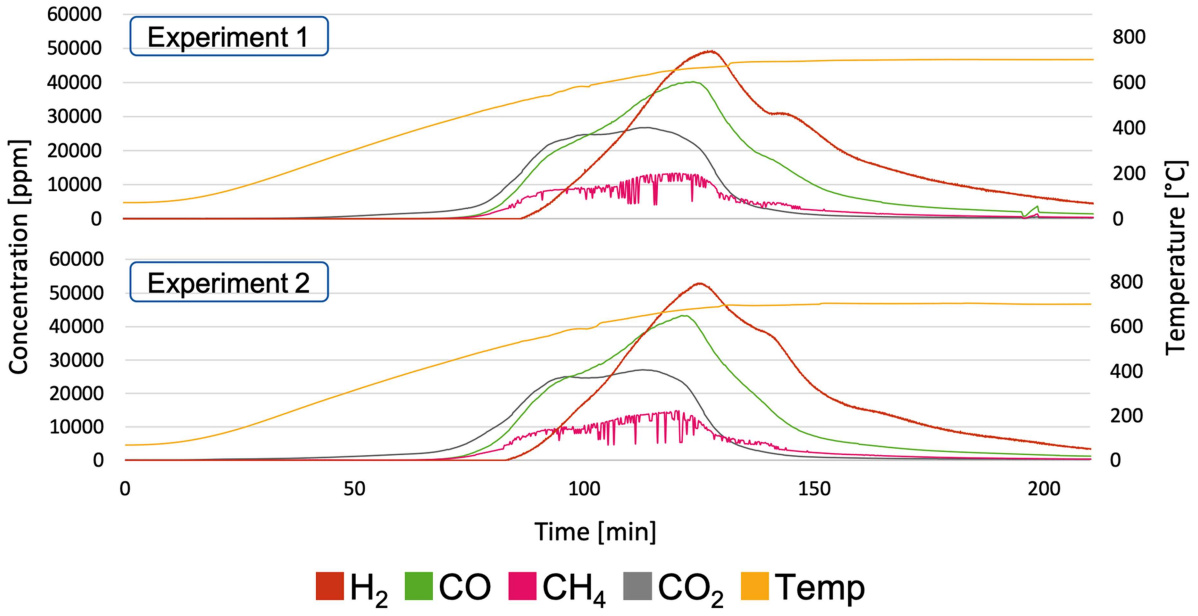


Figure 10. Degassing behaviour during the experiments for the Ultem 1000 reference material. The reference state is dry for all gas components.

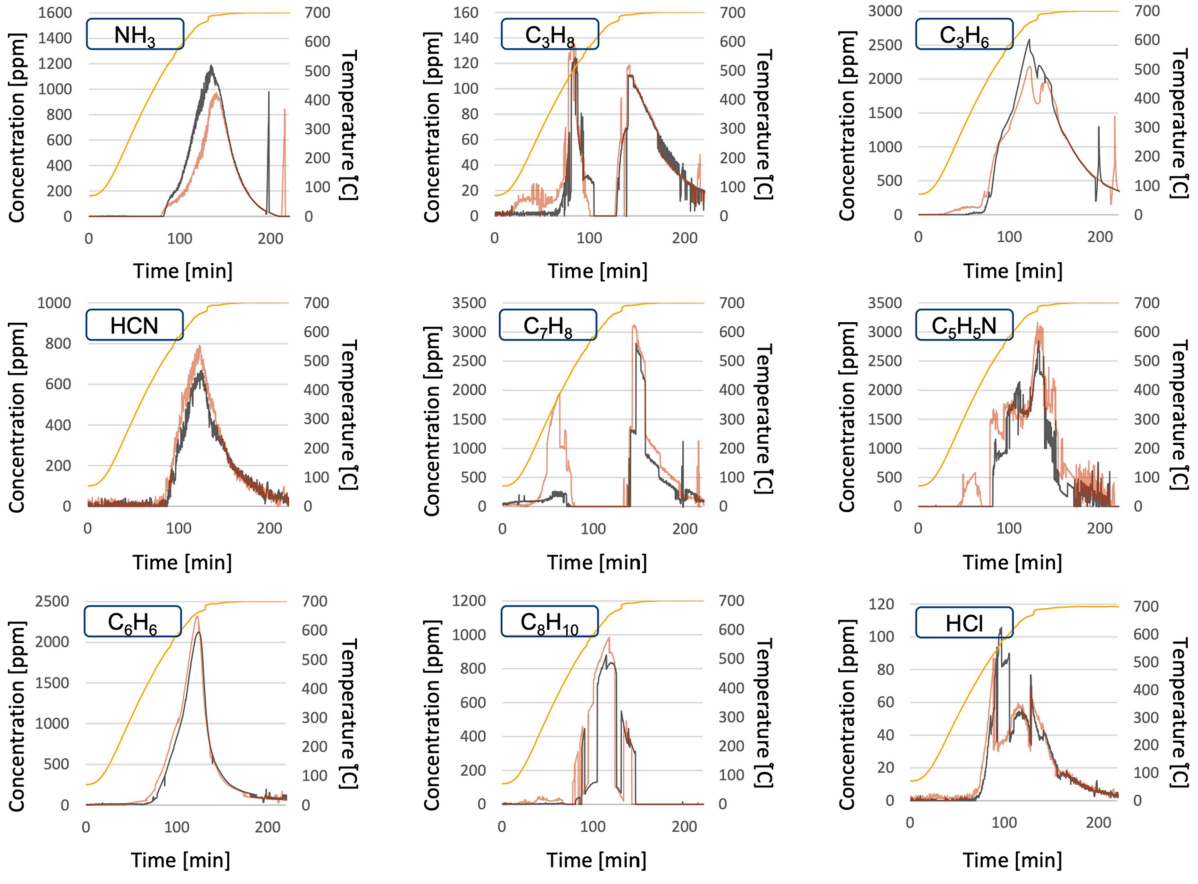


Figure 11. Minor gas components were detected via FTIR for the reference material. The reference state is dry for all gas components. Red: Experiment 1, grey: Experiment 2, yellow: temperature profile.

As previously noted, the formation of ethane, ethylene and acetylene occurred at small concentrations of below approximately 100 ppm.

Once again, the formation of HCl was observed at temperatures above approximately 400 °C. In comparison to the previous experiment, the concentration of HCl doubled (end-of-life Ultem approximately 40 ppm, Virgin-grade Ultem approximately 80 ppm), which supports the assumption that the HCl signal is related to the investigated material system rather than being caused solely by random measurement artefacts. Since virgin-grade material was used for the experiments, contamination from the usage of glues or paints can be ruled out. Therefore, it is reasonable to assume that the source of the chlorine lies within the material itself. However, without independent chlorine speciation, additive formulation data or analysis of additional material batches, the chlorine source cannot be assigned unambiguously. The result is therefore interpreted only as evidence that chlorine-containing species were released under the investigated conditions.

The chromatograms of the pyrolysis oils obtained are displayed in Figures 12 and 13. As previously observed with the end-of-life retaining clips, characteristic decomposition products such as amines, nitriles, phthalimides and others can be observed. A total of 2,146 peaks were obtained from the chromatogram of the pyrolysis oil from the first condensation unit. The pyrolysis oil of the second condensation unit contained fewer fragments with only 907 peaks identified. In contrast to the chromatogram from the end-of-life retaining clips, more intense peaks can be observed. It is assumed that this is due

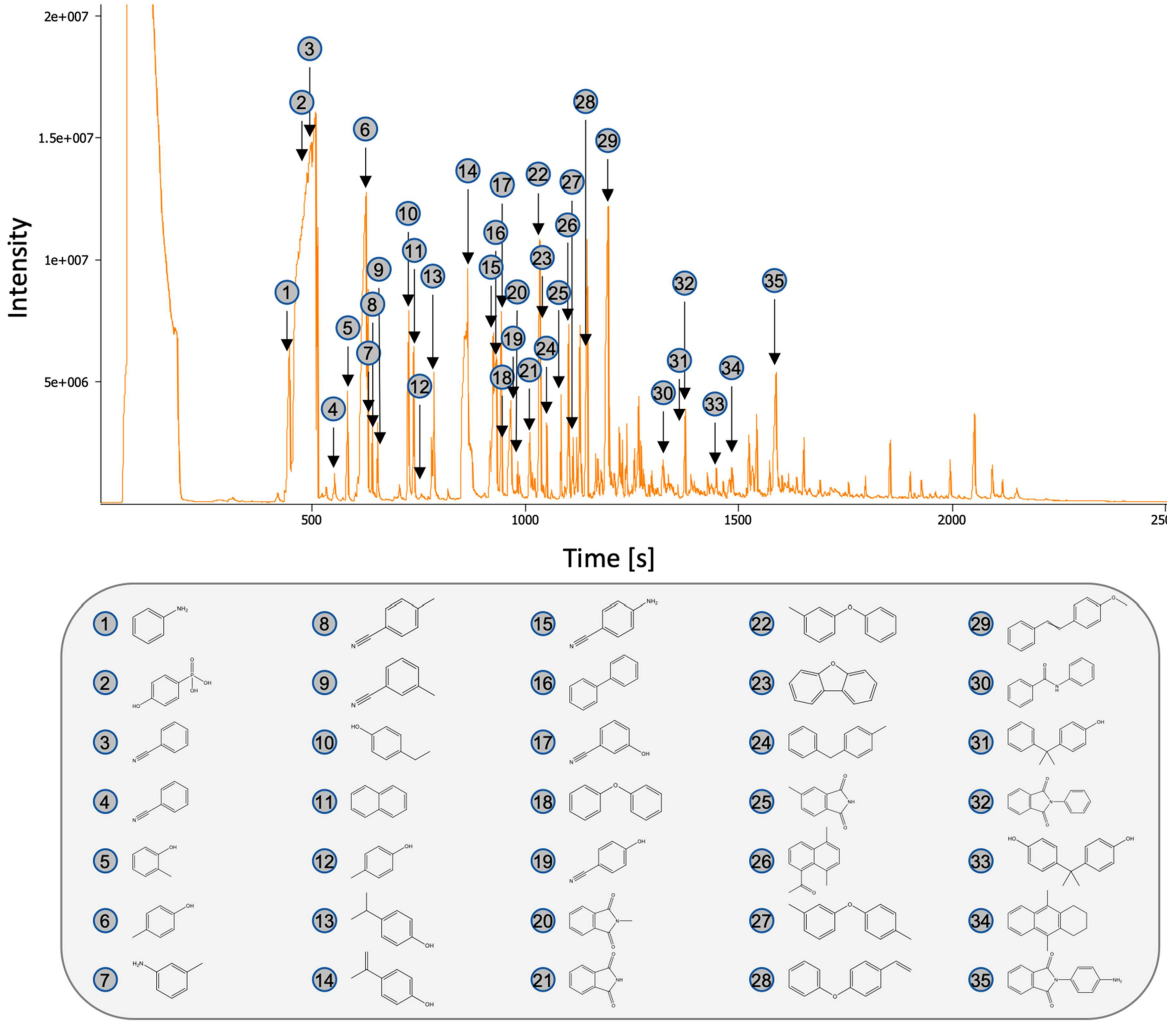


Figure 12. Chromatogram of the pyrolysis oil obtained from the first condensation unit for the Ultem 1000 reference material.

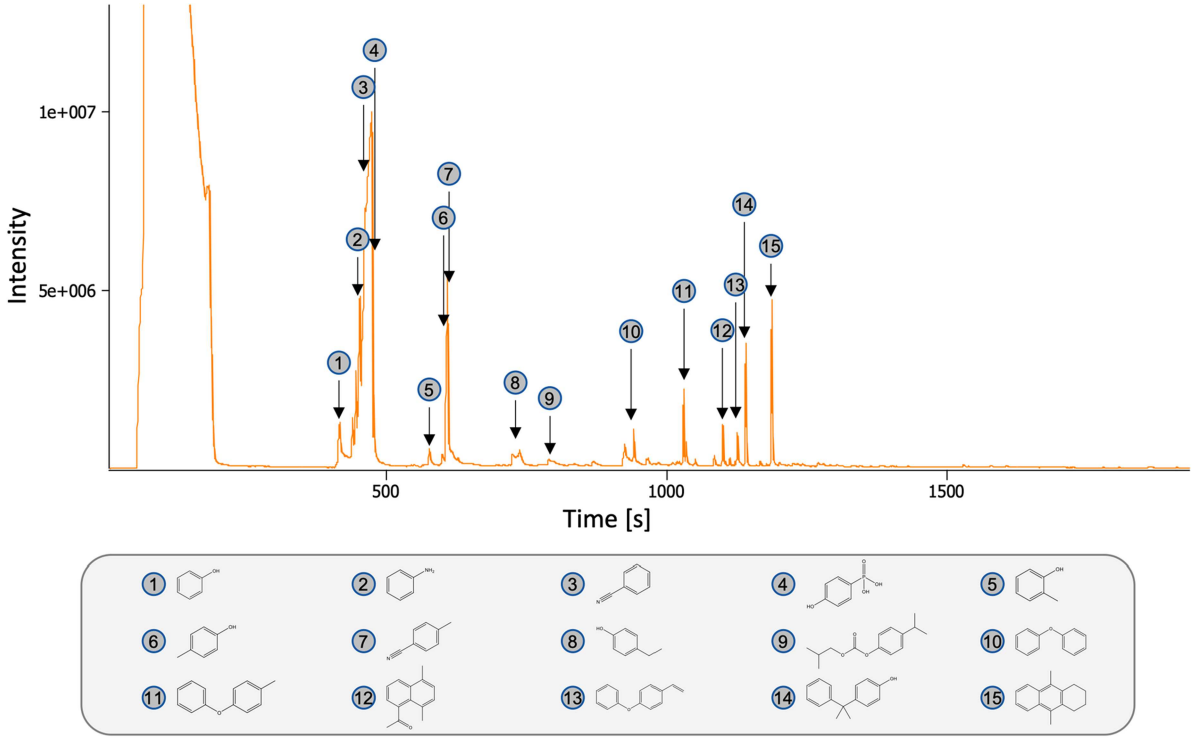


Figure 13. Chromatogram of the pyrolysis oil obtained from the second condensation unit for the Ultem 1000 reference material.

to the greater sample mass used for this material. Overall, the decomposition pattern was very similar. Again, a significant amount of (*p*-hydroxyphenyl)-phosphonic acid was found. As previously observed, the amount of benzene, toluene, ethylbenzene and xylenes is negligible; the concentration of bisphenol-A ranges from 19.7 to 59.87 mg L^{-1}. Overall, the condensates were again dominated by aromatic oxygen- and nitrogen-containing degradation products, particularly phenolic, nitrile- and imide-type compounds. Thus, despite the stronger signal intensity, the pyrolysis oils of the virgin-grade Ultem also showed no indication of a narrow or easily utilisable product spectrum for direct material recovery under the investigated conditions.

As previously noted, the condensates obtained were analysed regarding their carbon, hydrogen and nitrogen contents. The data obtained is displayed in Figure 14. While the hydrogen and nitrogen content is within the range of the previous experiment, with about 7%–8% of hydrogen and 2%–3% of nitrogen, the carbon content highly differs. An almost even distribution of carbon was found to be within all the samples except for the pyrolysis oil of the second condensation trap of the first experiment. The overall carbon content ranges from approximately 9% to 48%. As in the previous experiment, the comparatively large scatter of the carbon values limits their quantitative interpretability. The observed deviations may result from the high volatility and chemical inhomogeneity of the condensates as well as from analytical challenges during liquid sample handling. The elemental analysis of the oil phase is therefore considered indicative rather than fully quantitative.

4.3. Side panel

The composition of the pyrolysis gas formed during the experiments is displayed in Figure 15. In contrast to the previous, Ultem 1000-based materials, the CO_2-formation starts at significantly lower temperatures of approximately 180 °C. Furthermore, the formation of the other gas components equally begins at lower temperatures, ranging from approximately 260 °C for CO and CH_4 and approximately 400 °C for H_2. Additionally, the overall gas concentration is slightly lower when compared to the Ultem 1000 reference experiment, ranging in the area of the end-of-life retaining clip experiment. With approximately

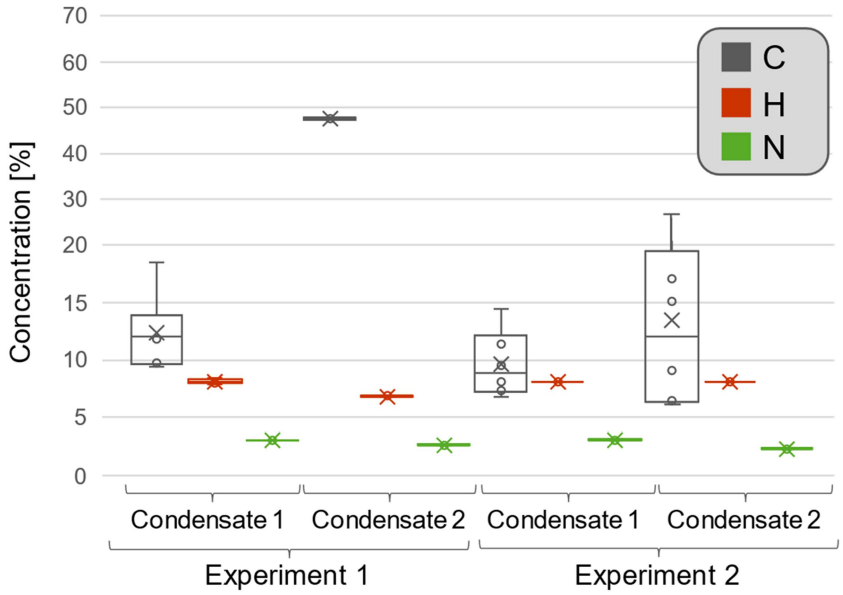


Figure 14. Ultimate analysis of the pyrolysis oils obtained from the Ultem1000 reference. The values refer to the reference state wet.

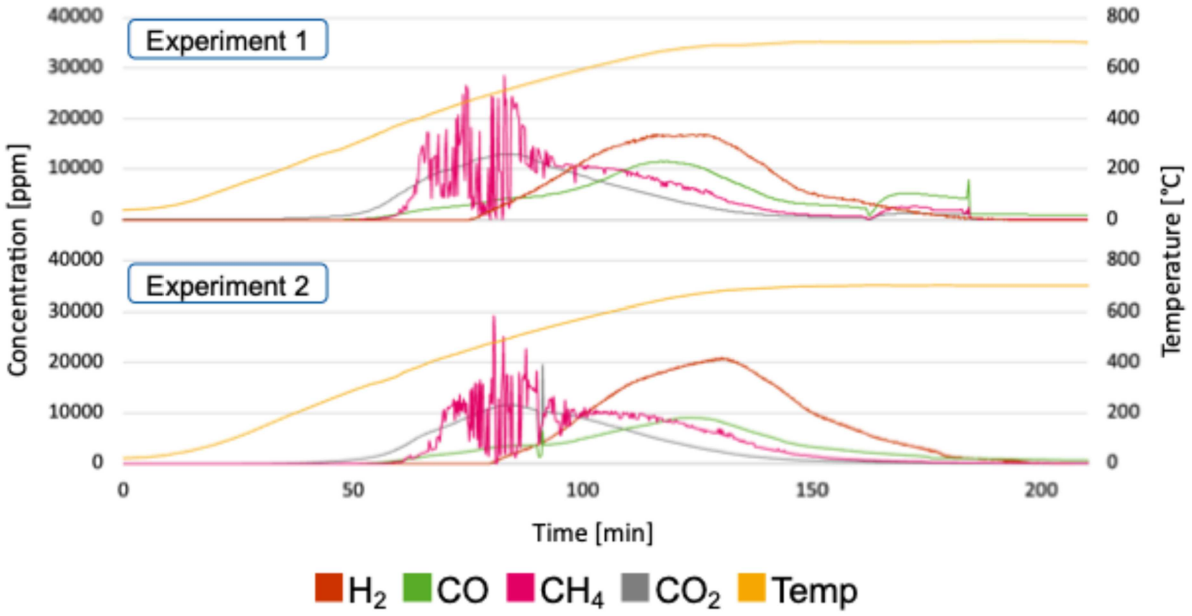


Figure 15. Degassing behaviour during the experiments for the side panel material. The reference state is dry for all gas components.

22.2%–24.3%, the amount of pyrolysis gas formed is lower in comparison with the Ultem 1000 reference experiment (30.2%–36.1%). This is due to the large amount of glass fibres within the sample used, which is reflected in the high ash content of this sample. The earlier onset of CO_2 and CO formation is consistent with the decomposition of oxygen-containing structures in the phenolic-resin-based material. As in the Ultem-based samples, CH_4 is likely formed from the cracking of smaller aliphatic fragments, whereas H_2 mainly originates from secondary high-temperature reactions of already formed volatile intermediates.

Additional components measured via FTIR are displayed in Figure 16. The majority of those compounds can be detected at temperatures of above approximately 280 °C. In contrast to the previous measurements, most of the gas concentration curves show very sharply defined steep increases. This

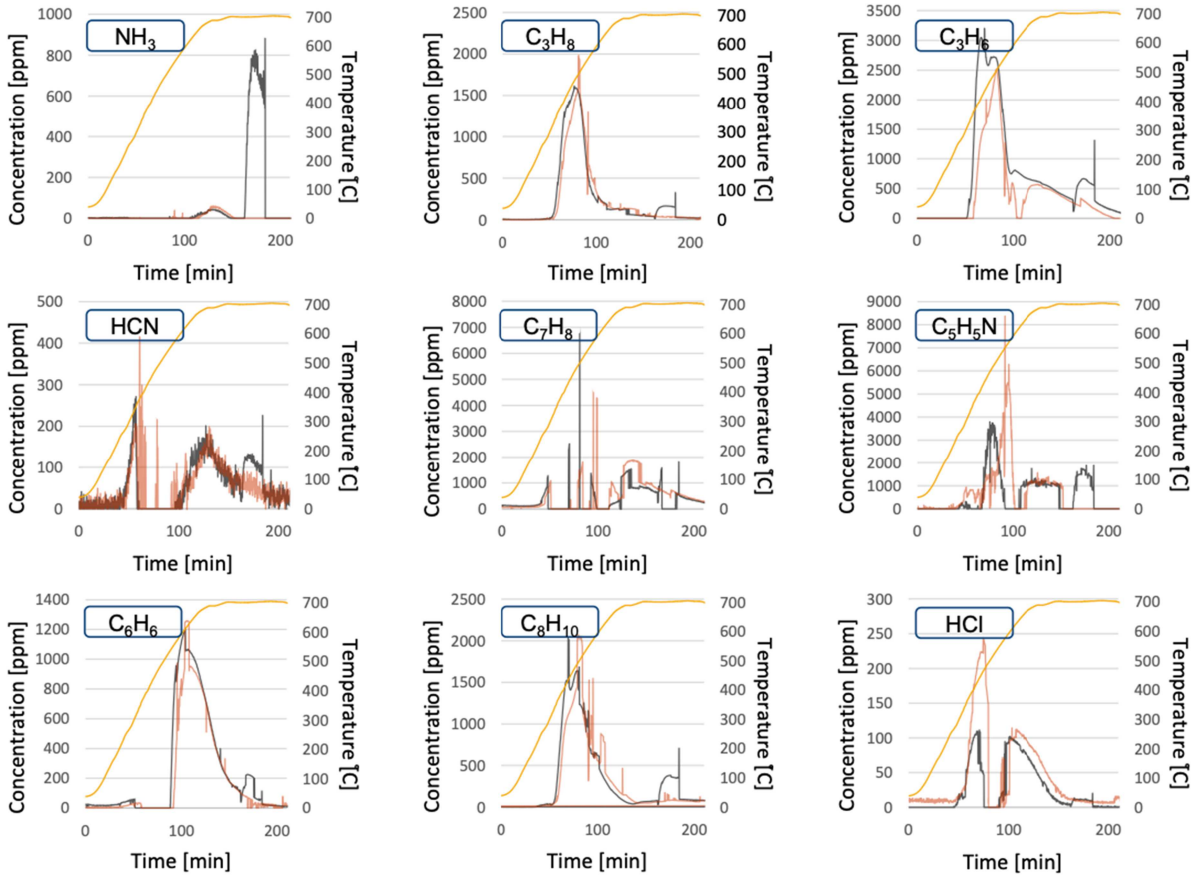


Figure 16. Minor gas components were detected via FTIR for the side panels investigated. The reference state is dry for all the gas components. Red: Experiment 1, grey: Experiment 2, yellow: temperature profile.

indicates that the formation of these substances occurs almost instantaneously when reaching the decomposition temperature. For propane and propene, these temperatures appear to be approximately 300 °C, for xylene at about 350 °C and for benzene at about 510 °C. Both toluene and pyridine show an erratic graph, indicating that the computer-based evaluation of the gas measurement was having difficulties identifying both substances. In comparison to the results of the Ultem 1000-based experiments, the formation of NH_3 commences at much higher temperatures of almost 700 °C and with significantly smaller concentrations. Furthermore, while the starting temperature of HCl formation is rather similar, the concentrations almost doubled. Additionally, it appears to be a two-stage degradation mechanism with the first degradation step at approximately 330 °C and the second degradation at approximately 600 °C. The detection of propane and propene again shows that small hydrocarbons are formed during decomposition, most likely by the cleavage and secondary cracking of aliphatic fragments associated with the resin matrix. Furthermore, the formation of ethane (up to approximately 800 ppm) and ethylene (up to approximately 1,350 ppm) was detected, while acetylene was rarely noticed. The comparatively low NH_3 concentrations indicate a smaller contribution of nitrogen-containing volatile products than in the Ultem-based samples, whereas nitrile and aromatic species remain important decomposition products. In combination with the chlorine and bromine detected in the solid residues, these findings suggest that halogen-containing constituents may be present in the side-panel material system. It is possible that this contamination originates from the paints and adhesives used to manufacture these parts. However, the exact chemical nature and origin could not be resolved within the scope of this study.

The pyrolysis oils obtained contained minor amounts of BTEX with approximately 0.32 mg/L^{-1} of benzene, 1.4 mg/L^{-1} toluene, 0.94 mg/L^{-1} ethylbenzene and 1.8 mg/L^{-1} xylenes. A significant amount of bisphenol-A was detected, ranging from 163.0 to 723.6 $mg\ L^{-1}$, representing the highest amount observed in the experiments conducted. The chromatograms of the pyrolysis oils showed distinctive fragments of the aramid and phenolic resins contained in the samples. The most prominent fragments contained

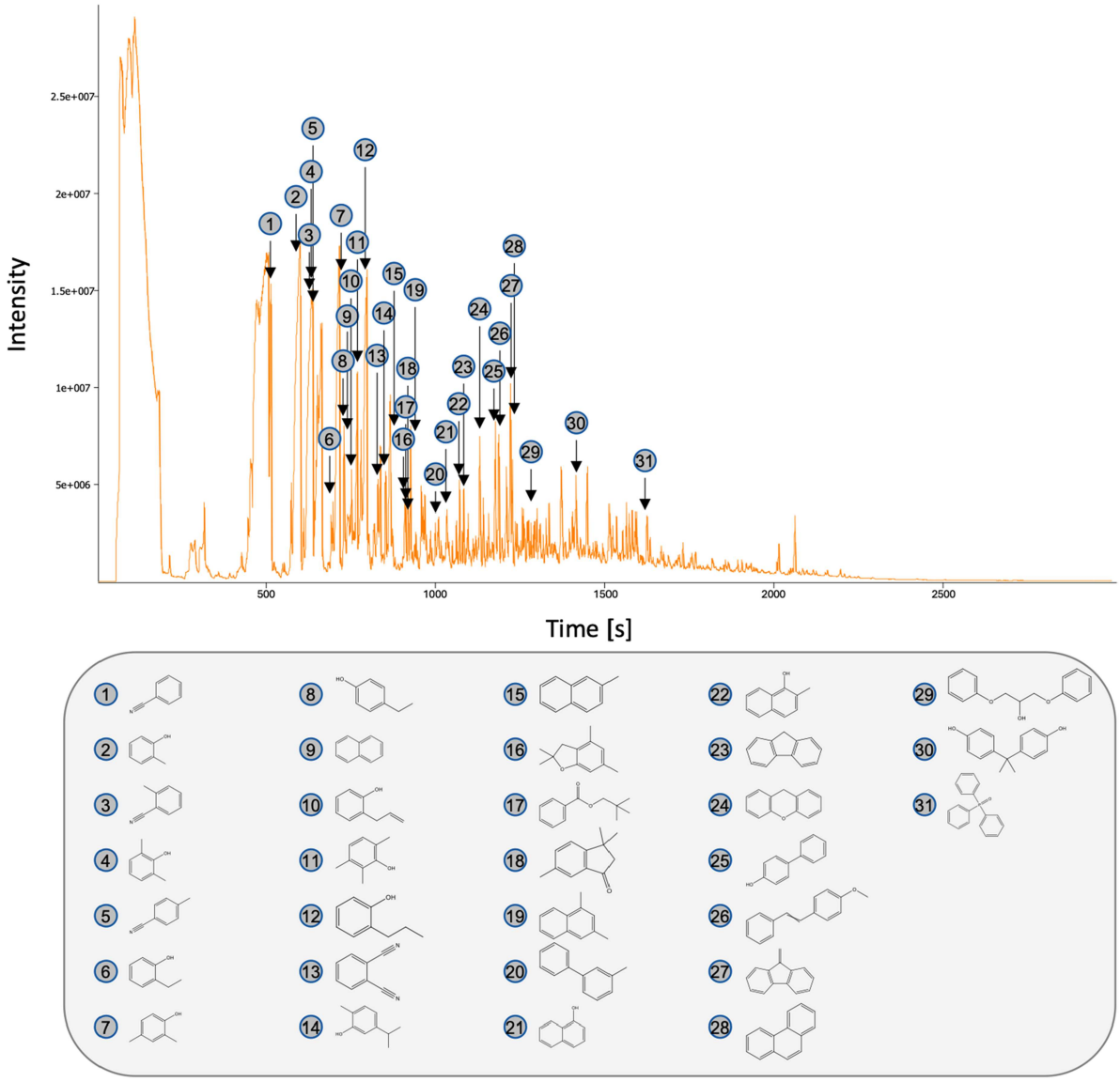


Figure 17. Chromatogram of the pyrolysis oil obtained from the first condensation unit for the side panels.

nitriles, phenols, amines and alcohols. The chromatogram of the first condensation unit contained 2,433 substances identified by the evaluation software, and the second condensation unit contained 2,294 components. The chromatograms obtained are displayed in Figures 17 and 18.

In contrast to the previously discussed (4-hydroxyphenyl)phosphonic acid found in the Ultem 1000-based pyrolysis oils, the amount of this substance was significantly lower in the oils obtained from the side panels. Instead, large amounts of triphenylphosphine oxide were observed, which can also be used as flame retardants. (Hastie 1973; Mariappan et al. 2013; Rakotomalala, Wagner, and Döring 2010) This difference indicates that, besides the polymer backbone itself, additive-related constituents also contribute to the composition of the condensates and further increase product heterogeneity.

The obtained condensates were analyzed regarding their carbon, hydrogen and nitrogen contents. The data obtained from the analysis are displayed in Figure 19. The hydrogen and nitrogen contents are once again very similar for both experiments conducted and range from 7.5% to 8.5% for hydrogen and from 0.8% to 1.4% for nitrogen. As previously observed, the carbon content has a large scatter in the measured values, ranging from approximately 5% to 40%. This again indicates the limited reproducibility of the elemental analysis for the condensate samples. As for the other materials, the results are likely influenced by the volatility and compositional inhomogeneity of the liquid products and should therefore be interpreted as approximate values only.

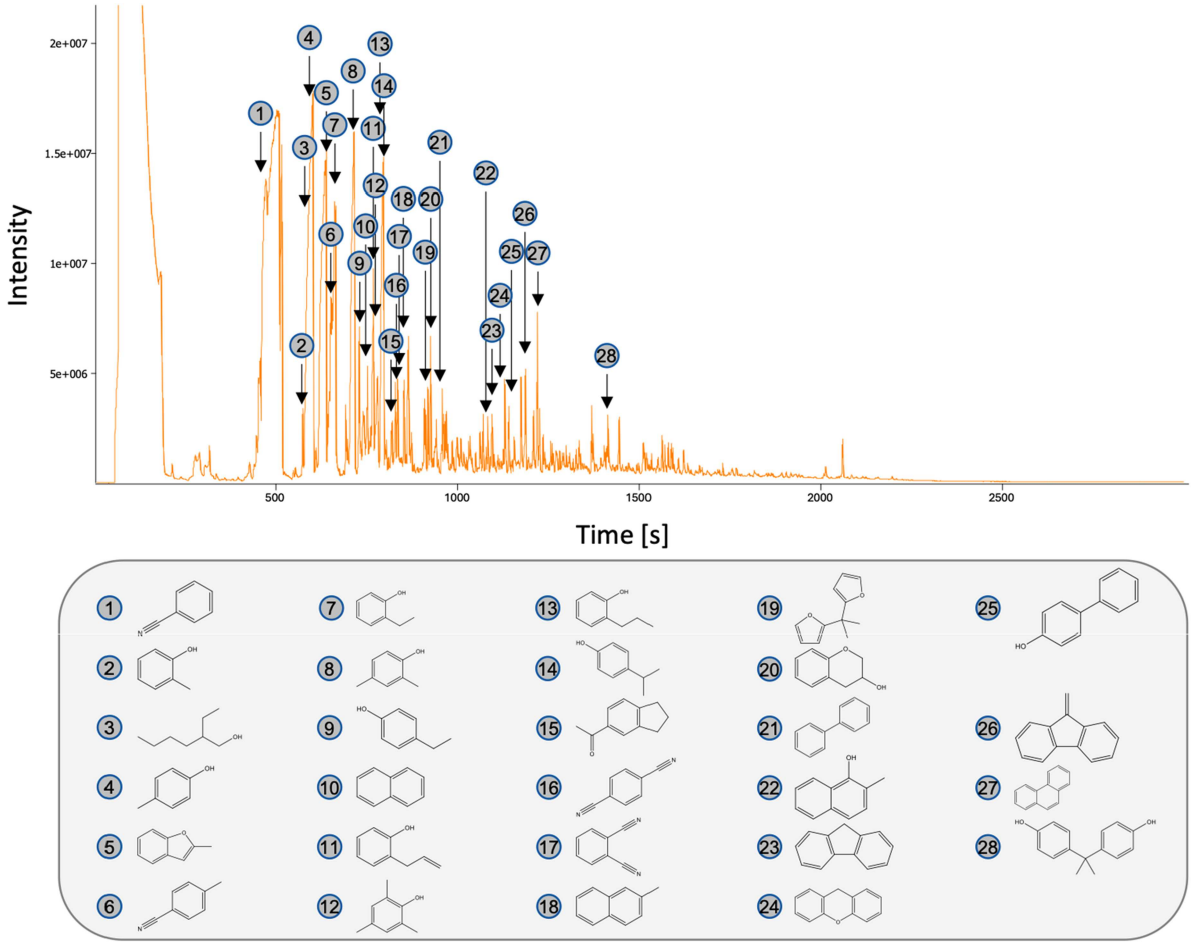


Figure 18. Chromatogram of the pyrolysis oil obtained from the second condensation unit for the side panels.

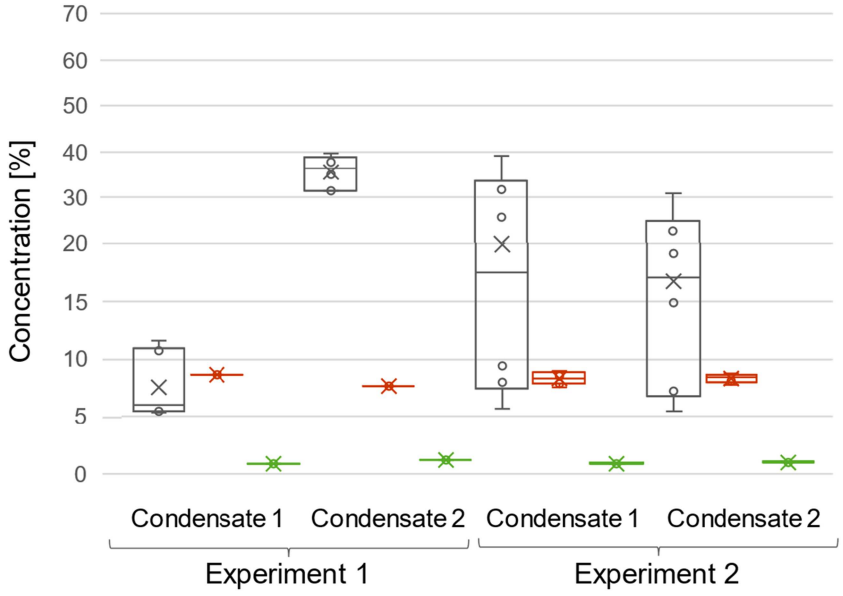


Figure 19. Ultimate analysis of pyrolysis oils obtained from the side panels. The values refer to the reference state wet.

4.4. Chars

The chars obtained in the experiments were analysed as described in Section 2.3. The chars originating from the retaining clips as well as the cabin side panel contain high amounts of ashes, whereas the char from the reference material has a very low ash content. Ultimate and proximate analyses of the chars produced are displayed in Table 3.

Interestingly, the chars obtained from the side panels contained comparably large amounts of chlorine, which is consistent with the HCl formation observed during pyrolysis. The exact origin of this chlorine remains unclear. Possible sources include chlorine-containing additives (e.g. flame retardants), surface treatments, adhesive-related constituents, or service-related residues. However, no unambiguous assignment can be made based on the present data.

The chars were furthermore examined microscopically to identify the structure of the glass fibres in the produced char. Figure 20 displays images from the microscope and highlights the glass fibres within the char. The retaining clips contained short fibre structures that blended into the char, creating an inseparable mixture. The fibre length was inhomogeneous, ranging from a few µm to approximately 250 µm. The char samples of the side panels showed a delaminating behaviour, separating the glass fibre structure from the Nomex-base while still blending both layers. A separation of both laminates seems to be possible, but not without significant loss of purity and, therefore, quality. The chars produced formed around the fibres, creating a structure that could not be dissolved mechanically.

Using XRF spectroscopy, the chars were analysed regarding their elemental composition. The data obtained are displayed in Table 4. Owing to the low ash content in the Ultem 1000 reference material, almost no elements besides carbon were found. The char obtained from the retaining clips contained mostly elements from the second group and group 14 of the periodic table (mostly Ca and Si). Similar

Table 3. Ultimate and proximate analyses of the chars formed during the experiments.

		Char retaining clip	Char Ultem 1000 reference	Char cabin side panel	Standard
Water	[%]	0.38	0.4	0.4	DIN EN ISO 18134-3
Ash		43.11	0.53	61.82	DIN 51719
C		52.1	91.5	34.8	DIN 51732
H		0.82	1.67	0.65	DIN 51732
N		1.65	2.45	1.09	DIN 51732
Cl		<0.02	<0.05	0.53	DIN 51727
LHV	[MJ/kg]	18.78	33.35	12.34	DIN 51900

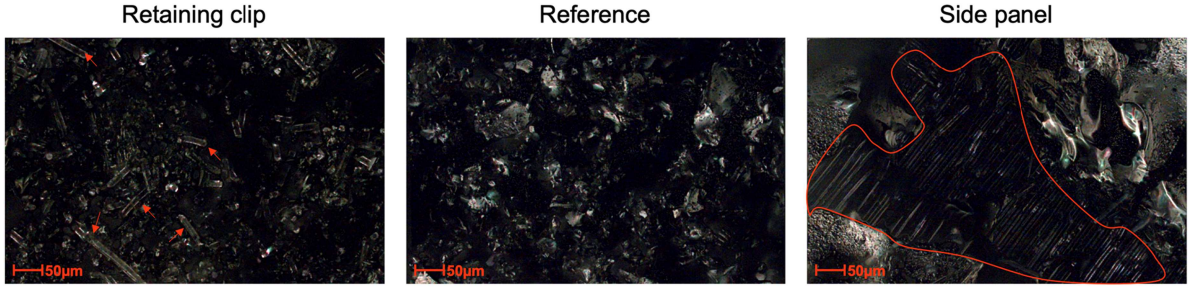


Figure 20. Microscope images of the produced chars. The red markers indicate the glass fibre structures.

Table 4. Summary of the data obtained by XRF spectroscopy of the chars obtained.

Group periodic table		Char retaining clip	Char Ultem 1000 reference	Char cabin side panel
1	[%]	0.67	0.39	0.84
2		6.98	0.03	9.97
3–12		0.036	0.09	12.51
13		1.67	0.02	3.23
14		9.30	0.06	10.49
15		0.03	0.01	0.04
16		0.01	0.01	0.06
17		0.02	0.04	0.99

values were detected for the char from the side panels, but the total amount was greater. Furthermore, this sample contained high amounts of titanium, but the origin of this metal remains unclear. Additionally, this sample contained significant amounts of bromine (up to 1.17%), which indicates the presence of bromine-containing constituents in the side-panel material system. A contribution from brominated flame-retardant additives is plausible, but cannot be confirmed without targeted additive analysis or formulation data.

4.5. Study limitations

This study was designed as a laboratory-scale feasibility assessment and therefore has several limitations. The pyrolysis experiments were conducted in duplicate, which allowed evaluation of the general reproducibility of the product yields and gas-evolution trends. However, the limited number of experimental replicates does not provide sufficient statistical power for a detailed comparison of small differences between individual materials or gas concentration peaks. The batch muffle furnace does not reproduce the heat- and mass-transfer conditions of continuous industrial reactors, which requires a separate evaluation because of the fundamentally different reaction conditions. In addition, non-target GC–MS was used primarily for qualitative identification of dominant compound classes, while quantitative conclusions for the condensates were restricted to targeted analyses. Elemental analysis of the liquid fractions should be interpreted as indicative because of low sample amounts, volatility and possible phase inhomogeneity. The studies did not include catalyst screening, process optimisation, life-cycle assessment, techno-economic assessment or systematic evaluation of collection logistics. Conclusions regarding industrial feasibility are therefore limited to the investigated process configuration and should be validated in larger-scale studies.

5. Conclusions

The pyrolysis experiments conducted in this study provided detailed insights into the thermal decomposition behaviour and product formation of selected aircraft cabin materials. All the investigated materials showed high thermal stability and predominantly formed solid residues (58.9%–71.8%) and permanent gases (21.7%–36.1%), whereas the yields of condensable products remained comparatively low. The condensates accounted for only 4.0%–8.2% of the initial sample mass and exhibited a highly complex chemical composition comprising a broad range of aromatic, oxygen- and nitrogen-containing compounds. These findings indicate that, under the investigated process conditions, direct material recovery through the utilisation of pyrolysis oils has limited technical attractiveness. A homogeneous chemical composition, low amounts of hydrocarbons with heteroatoms and a high yield of oils are generally required in order to achieve stable and reliable process conditions in follow-up processes. The pyrolysis oils obtained did not meet these criteria, as they consisted of highly heterogeneous hydrocarbon mixtures. When focusing on the energetic usage, the composition of the oils is less important, but the yield appears to be insufficient. Furthermore, the technical implementation of pyrolysis of end-of-life aircraft cabin parts requires permanent local availability, which in turn requires a collection strategy that transcends manufacturers and operators. Under the conditions investigated, the current low availability of material streams, low oil yields, and the large energy demand for pyrolysis make it seem very unlikely to implement these materials into a chemical recycling loop. While the usage of catalysts may increase the desired yields of oils or gases, their utilisation is commonly rather expensive. Furthermore, as the pyrolysis represents a two-phase-system (solid/gas, heterogeneous catalysis), the contact surface as well as the contact time between the catalyst and the feedstock itself is limited, reducing the likelihood of significant increases in oil-yields. In this context, Vastyl et al. reported the microwave-assisted catalytic pyrolysis of polyetherimide, achieving gas yields of up to approximately 80%, mostly consisting of hydrogen (approximately 40%–50%) and carbon monoxide (approximately 35%–45%). The yield of the condensates was comparable to the values reported in this work. The limiting factors in the approach published were a high catalyst loading of 1:1 (weight ratio) combined with a highly heterogeneous oil/wax composition (Vastly, Hill, and Lestinsky 2026).

From an engineering perspective, the observed product distribution has important consequences for the practical implementation of pyrolysis processes for aircraft cabin waste. Owing to the low liquid yields and

the high chemical heterogeneity of the condensates, an industrial process would not primarily be designed for pyrolysis-oil recovery. Instead, process concepts would have to focus on the utilisation of gaseous products, heat integration, reliable treatment of heteroatom-containing emissions and appropriate management of solid residues. The high char yields observed for the fibre-reinforced cabin components are particularly relevant in this context. The resulting residues consist of carbonaceous material, fibres, ash and inorganic constituents and would require further processing, utilisation or disposal.

With the state-of-the-art disposal of these components (at least in Europe), usually being the thermal utilisation (for example, in cement kilns) (Celikel, Rötger, and Casas 2022), the present results do not indicate that pyrolysis is a promising alternative pathway for direct chemical recycling of these materials under the investigated conditions. The current use of these materials in energy recovery represents an established disposal route, as it reduces the need for fossil-based energy carriers and is in accordance with European environmental laws (European Parliament 2008). Furthermore, modern flue gas cleaning systems ensure the elimination of potentially harmful substances from the fumes, ensuring safe operations. Nevertheless, the incineration of this waste stream results in the loss of material for future recycling processes.

At the same time, the results indicate that alternative recovery routes may be more promising for specific fractions of aircraft cabin waste. For comparatively clean, Ultem-rich fractions, solvent-based or solvolytic recycling approaches may warrant further investigation (Keith et al. 2025), whereas for mixed or highly contaminated fractions, gasification could represent an alternative thermochemical recovery route. These options were not investigated in the present study and therefore require separate assessment.

Acknowledgements

This study was supported by Diehl Aviation Laupheim GmbH through the provision of the end-of-life components.

Author contributions

CRediT: **Clemens Schmittmann:** Conceptualization, Data curation, Formal analysis, Funding acquisition, Investigation, Methodology, Project administration, Resources, Supervision, Validation, Visualization, Writing – original draft, Writing – review & editing; **Kai Schlögel:** Data curation, Methodology, Resources, Validation, Writing – review & editing; **Fabian Roemer:** Formal analysis, Investigation, Validation, Visualization, Writing – review & editing; **Kevin Carl:** Funding acquisition, Project administration, Resources, Writing – original draft; **Peter Quicker:** Conceptualization, Funding acquisition, Methodology, Project administration, Supervision, Validation, Writing – review & editing.

Disclosure statement

No potential conflict of interest was reported by the author(s).

Funding

This research was funded by the Federal Ministry of Economic Affairs and Climate Action of Germany, Grant number 20K2205C.

Data availability statement

The data presented in this study is available under: https://10.4121/b8da8bcb-85f5-4cc1-a669-123ed6d12ea5.

Biographical note

N/A.

References

Bachmann, J., X. Yi, K. Tserpes, C. Sguazzo, L. G. Barbu, B. Tse, C. Soutis, E. Ramón, H. Linuesa, and S. Bechtel. 2021. "Towards a Circular Economy in the Aviation Sector Using Eco-Composites for Interior and Secondary Structures. Results and Recommendations from the EU/China Project Eco-Compass." *Aerospace* 8: 131. https://doi.org/10.3390/aerospace8050131.

Celikel, A., T. Rötger, and G. Casas. 2022. Assessment of the Environmental Sustainability Status in the Aviation Maintenance and Production Organisation (M&P) Domain In *Envisa*. European Union Aviation Safety Agency. https://www.easa.europa.eu/sites/default/files/dfu/study_-_assessment_of_the_environmental_sustainability_status_in_the_aviation_maintenance_and_production_organisation_mp_doma.pdf Accessed on 09.12.2025.

Clark, R. A. , and M. P. Shaver. 2024. "Depolymerization Within a Circular Plastics System." *Chemical Reviews* 124: 2617–2650. https://doi.org/10.1021/acs.chemrev.3c00739.

European Parliament. 2008. Directive /98/ECOfficial Journal oft he European Union 2008 2025. http://data.europa.eu/eli/dir/2008/98/oj.

Hastie, J. W. 1973. "Molecular Basis of Flame Inhibition." *Journal of Research on the National Bureau of Standards – A. Physics and Chemistry*. 77.

Keith, M. J., B. Al-Duri, T. O. McDonald, and G. A. Leeke. 2025. "Solvent-Based Recycling as a Waste Management Strategy for Fibre-Reinforced Polymers: Current State of the Art." *Polymers* 17: 843. https://doi.org/10.3390/polym17070843.

Luo, H., H. Tyrrell, J. Bai, R. I. Muazu, and X. Long. 2024. "Fundamental, Technical and Environmental Overviews of Plastic Chemical Recycling." *Green Chemistry* 26: 11444. https://doi.org/10.1039/d4gc03127j.

Mariappan, T., Z. You, J. Hao, and C. A. Wilkie. 2013. "Influence of Oxidation State of Phosphorus on the Thermal and Flammability of Polyurea and Epoxy Resin." *European Polymer Journal* 49 (10). https://doi.org/10.1016/j.eurpolymj.2013.06.009.

Naqvi, S. R., Mysore Prabhakara, H. Bramer, E. A. Dierkes, W. Akkerman, and R. Brem. 2018. "G. a Critical Review on Recycling of End-Of-Life Carbon Fibre/Glass Fibre Reinforced Composites Waste Using Pyrolysis Towards a Circular Economy." *Resources, Conservation & Recycling* 136. https://doi.org/10.1016/j.resconrec.2018.04.013.

National Research Council. 1995. Fire- and Smoke-Resistant Interior Materials for Commercial Transport AircraftWashington, DC: The National Academies Press. https://doi.org/10.17226/5073.

Pahnila, M., A. Koskela, P. Sulasalmi, and T. Fabritius. 2023. "A Review of Pyrolysis Technologies and the Effect of Process Parameters on Biocarbon Properties." *Energies* 16: 6936. https://doi.org/10.3390/en16196936.

Qureshi, J. 2022. "A Review of Recycling Methods for Fibre Reinforced Polymer Composites." *Sustainability* 14: 16855. https://doi.org/10.3390/su142416855.

Qureshi, J. 2022. "A Review of Recycling Methods for Fibre Reinforced Polymer Composites." *Sustainability* 14: 16855. https://doi.org/10.3390/su142416855.

Rakotomalala, M., S. Wagner, and M. Döring. 2010. "Recent Developments in Halogen Free Flame Retardants for Epoxy Resins for Electrical and Electronic Applications." *Materials* 3: 4300–4327. https://doi.org/10.3390/ma3084300.

Sonnier, R., B. Otazaghine, C. Vagner, F. Bier, J.-L. Six, A. Durand, and H. Vahabi. 2019. "Exploring the Contribution of Two Phosphorus-Based Groups to Polymer Flammability Via Pyrolysis–Combustion Flow Calorimetry." *Materials* 12: 2961. https://doi.org/10.3390/ma12182961.

Stanfield, M. K., J. Carrascal, L. C. Henderson, and D. J. Eyckens. 2021. "α-Aminophosphonate Derivatives for Enhanced Flame Retardant Properties in Epoxy Resin." *Materials* 14: 3230. https://doi.org/10.3390/ma14123230.

Vastly, M., J. M. Hill, and P. Lestinsky. 2026. "Microwave-Assisted Catalytic Decomposition of Polyetherimide with a Focus on Hydrogen and High-Value Hydrocarbons Production." *Journal of Environmental Chemical Engineering* 14 (3). https://doi.org/10.1016/j.jece.2026.122233.

Wong, K., C. Rudd, S. Pickering, and X. Liu. 2017. "Composites Recycling Solutions for the Aviation Industry." *Science China Technological Sciences* 60: 1291–1300. https://doi.org/10.1007/s11431-016-9028-7.

Yousef, S., J. Eimontas, N. Striugas, M. Praspaliauskas, and M. A. Abdelnaby. 2021. "Pyrolysis Kinetic Behaviour of Glass Fibre-Reinforced Epoxy Resin Composites Using Linear and Nonlinear Isoconversional Methods." *Polymers* 13: 1543. https://doi.org/10.3390/polym13101543.

Zhou, R., W. Li, J. Mu, Y. Ding, and J. Jiang. 2020. "Synergistic Effects of Aluminum Diethylphosphinate and Melamine on Improving the Flame Retardancy of Phenolic Resin." *Materials* 13: 158. https://doi.org/10.3390/ma13010158.